Journal of Molecular Graphics and Modelling 28 (2010) 598–603

Contents lists available at ScienceDirect

Journal of Molecular Graphics and Modelling

journal homepage: www.elsevier.com/locate/JMGM

The phosphorylation specificity of B-RAF^{WT}, B-RAF^{D594V}, B-RAF^{V600E} and B-RAF^{K601E} kinases: An *in silico* study

Filip Fratev *, Svava Ósk Jónsdóttir

Center for Biological Sequence Analysis, Department of Systems Biology, Technical University of Denmark, Kemitorvet, Building 208, DK-2800 Kongens Lyngby, Denmark

ARTICLE INFO

Article history:
Received 9 July 2009
Received in revised form 14 December 2009
Accepted 15 December 2009
Available online 24 December 2009

Keywords:
B-RAF
B-RAF^{V600E}
GRID
Molecular dynamics
Kinase

ABSTRACT

Phosphorylation of the B-RAF kinase is an essential process in tumour induction and maintenance in several cancers. Herein the phosphorylation specificity of the activation segment of the wild type B-RAF kinase and the B-RAF^{D594V}, B-RAF^{V600E} and B-RAF^{K601E} mutants was examined by molecular dynamics (MD) simulations and GRID molecular interaction field analysis. According to our analysis, Thr599 and Ser602 were the only residues in the activation segment in B-RAF^{WT} that were well exposed to ATP binding, which is in agreement with the experimental results, and provide a molecular basis of the observed phosphorylation. The phosphorylation specificity was altered significantly for each of the three different mutants studied due to the large conformational changes and subsequent alterations in the electrostatic forces between several residues for each of these mutants. Thus the analysis revealed limited phosphorylation potential of the non-active B-RAF^{D594V} mutant and several potential ATP binding sites were identified for the highly active B-RAF^{V600E} mutant.

The Lys601 residue, which is specific to RAF and not present in the activation segment of other similar kinases, was identified to potentially be of major importance to the observed differences in the phosphorylation specificity of the mutants. Our results indicate that Lys601 might be a specific ATP coordinating residue, contributing to the B-RAF phosphorylation specificity. The overall results can be helpful for the understanding of the B-RAF phosphorylation processes on a molecular level.

1. Introduction

The RAF–MEK–ERK signal transduction cascade is a conserved protein pathway that regulates cell growth, differentiation, and proliferation in response to external stimuli (growth factors, cytokines, or hormones) [1]. When B-RAF is activated it activates the protein kinase MEK, which in turn activates a third protein kinase called ERK. As phosphorylation of the B-RAF kinase is a vital process to mediate it's activation, better understanding of ATP binding in the wild type B-RAF and key mutations is essential. Clinically, it has been determined that ~66% of melanomas, ~36% of thyroid tumours, and ~10% of colon cancers in humans can be correlated with mutations that have occurred in the B-RAF kinase domain [2]. Thus, B-RAF has been considered as an attractive new drug target.

It has been experimentally established that the activation of wild type B-RAF (B-RAF^{WT}) requires phosphorylation of the activation segment (named A-loop here) at the Thr599 and/or Ser602 residues [3]. It has been suggested that these two residues are those most exposed to ATP molecules [4], but there is still neither available experimental nor theoretical arguments that support this hypothesis. It was proposed that the V600E mutation mimics the phosphorylation step and can activate MEK directly and subsequently stimulate ERK without phosphorylation taking place [2,5]. GLU600 is considered to acts as a phosphomimetic between the Thr599 and Ser602 phosphorylation sites, inducing conformational change in the protein structure [6]. It was speculated that most of the other activating B-RAF mutants mimic the phosphorylation step as well [5,6]. However, experimental data for the phosphorylation specificity of the activation segment is only available for the wild type B-RAF, and thus sufficient data to support this hypothesis is not yet available. Moreover, it has been shown that the activated B-RAF^{V600E} binds to an Hsp90–cdc37 protein complex. It is reported that this process is required for the B-RAF^{V600E} stability, function and the evolution of the melanomas and the other tumours that depend on this mutation [7].

A significant number of mutations of B-RAF are reported; most of them with elevated activity compared to the basal one, but four mutants have impaired kinase activity [5]. Three of the impaired activity mutants are only capable of inducing ERK phosphorylation through heterodimerization with C-RAF. The fourth mutant, B-RAF^{D594V}, acts like a kinase-dead mutant and cannot bind to C-RAF. Its role in tumorigenesis remains to be elucidated [8].

* Corresponding author. Tel.: +45 45252477; fax: +45 45931585.
E-mail addresses: fratev@cbs.dtu.dk (F. Fratev), svava@cbs.dtu.dk (S. Jónsdóttir).

1093-3263/$ – see front matter © 2009 Elsevier Inc. All rights reserved.
doi:10.1016/j.jmgm.2009.12.005

Asp594 is a key catalytic residue for many kinases, and thus it is not surprising that B-RAF^{D594V} is a loss-of-function mutant [9,10]. However, the impact of the D594V and several other mutations on the conformation of residues that can potentially interact with ATP, such as Lys483, Glu501 and Asp594, and how the different mutations influence the phosphorylation specificity and the activation of the different mutants, is yet unclear. Also, the role of phosphorylation in the activation of strongly activating B-RAF mutants, such as V600E and K601E, is not well understood [5,11].

The crystal structures of the inactive B-RAF^{WT} and B-RAF^{V600E} kinase binding domains in a complex with the inhibitor Sorafenib (BAY-439006) have been published [5] and recently the structures of the active B-RAF form were solved as well [12–14], adding to the understanding of these type of kinases. However, a significant portion of the activation segment, which plays an essential role in phosphorylation and kinase activation, was not solved in any of the available structures.

The purpose of this study is to analyse the phosphorylation specificity of B-RAF^{WT} and three key mutants (B-RAF^{V600E}, B-RAF^{D594V} and B-RAF^{K601E}) and to gain improved understanding of the underlying molecular basis for experimentally measured activity deviations. The full structural models of these four B-RAF forms were based on the available crystal structures, supplemented by models for the missing A-loop portions [15,16]. The structures were refined by 15 ns molecular dynamics simulations, and the phosphorylation specificity of each kinase was analysed with the GRID method. Previous studies of the effect of the different mutations on especially the electrostatic interactions and on the formation of networks of hydrogen bonds within the binding cavity were used to provide additional support to our results [15,16].

2. Methods

2.1. Preparation of protein structures

Before carrying out the MD simulations and the GRID analysis, the structures of B-RAF^{WT}, B-RAF^{V600E}, B-RAF^{K601E} and B-RAF^{D594V} were prepared as previously described [15]. For the two B-RAF forms, B-RAF^{WT} and B-RAF^{V600E}, for which crystal structures were available in the protein data bank [17] (pdb codes: 1uwh and 1uwj), the structures were prepared by removing the inhibitor Sorafenib and keeping the crystal waters. Those A-loop residues not solved in the crystal structures, residues 601–612 and 603–614 in B-RAF^{WT} and B-RAF^{V600E}, respectively, were modelled with the Modeller software [18]. The mutants B-RAF^{K601E} and B-RAF^{D594V} were constructed by substituting the original residues of the crystal structure of B-RAF^{WT} with the appropriate amino acids, respectively. The A-loop region was modelled and refined in the same way as for the two other B-RAF forms.

2.2. Molecular dynamics

To obtain sufficiently accurate structures for the GRID analyses, we used structures obtained from a series of 15 ns MD simulations of the wild type kinase and the studied B-RAF mutants [16]. Before initiating the MD simulation, the complexes were prepared with the Amber 9 software [19] and subsequently the MD simulations were carried out with NAMD v.2.6 [20]. The simulated systems were placed in the centre of a truncated octahedron simulation box filled with water molecules, which were represented with the SPC/E water model [21]. The buffering distance was set to 10 Å. Counter ions were added to maintain the electro neutrality of the complexes. The Amber 2003 force field was employed for the simulations [19]. All systems were energy minimized in two steps. First only the waters and ions were minimized for 2000 steps keeping the protein fixed. A second minimization was then performed on the whole system for 8000 steps with the conjugate gradient method to convergence criterion of 0.5 kcal mol^{-1} Å^{-1}. Initially, the simulation complexes were gradually heated from 0 to 300 K for 30 ps (NTV), further equilibrations for a 200 ps were performed, followed by production runs of 15 ns (NTP). Langevin dynamics was utilized to keep a constant temperature. Constant pressure of 1 atm was imposed using the hybrid Nosé–Hoover Langevin piston method with a decay period of 200 fs and a damping time-scale of 50 fs. The non-bonded cut-off was set to 12.0 Å. The SHAKE algorithm was applied for all bonds involving hydrogen atoms [22]. A 2 fs integration time step was used, and long-range electrostatic interactions were treated with the particle-mesh Ewald (PME) method [23]. Data were collected every 500 steps, i.e., every 1 ps. The calculation of the root-mean-square deviations (RMSD) and the corresponding standard deviations (SDs) were carried out with the VMD package and its Tcl routine [24].

2.3. GRID calculations

In order to indentify the possible ATP binding sites and to obtain detailed understanding of the forces contributing to the phosphorylation specificity of the studied B-RAF forms, a series of calculations were performed with the GRID program, version 22 [25,26]. The three-dimensional structures for each of the B-RAF forms obtained from the 15 ns MD simulations [16] were imported into the GRID program, and the non-covalent interactions between the proteins residues and small chemical groups, so-called probes, were calculated. By generating a grid net in the proteins binding pocket and placing a probe at each grid point, a set of interaction energies between the probe and the surrounding protein residues are calculated.

Thus, in order to indentify those residues that might react with a phosphate group provided by ATP, i.e. residues that can potentially undergo phosphorylation, a PO_4H group was used as probe. To obtain greater understanding on how the electrostatic forces induced by the ATP molecule affect ATP transport and binding, a negative charge of −3 was used as probes as well. These two probes where thus used to generate a virtual reaction between ATP and the protein residues in order to mimic the phosphorylation process within the B-RAF binding site.

GRID maps were used to identify and graphically illustrate the favoured ATP binding sites of the kinases. A cut-off value was introduced, and regions with protein–probe interactions energies that are more negative or equal to −15.0 kcal/mol are shown. The graphs were then used to identify residues that exhibit strong protein–probe interactions.

For each the B-RAF forms, the GRID calculation was done by centring the box on the proteins centre with sufficient dimensions to accommodate the proteins. A grid box of density one point per 1 Å was used, and the interactions between the protein and the two selected probes were evaluated by placing the respective probes at each grid point.

3. Results and discussion

3.1. Molecular dynamics

Detailed analysis of the MD simulations that form basis for the GRID calculations is presented in a separate publication [16]. The mean RMSD of the backbone proteins atoms during the simulation period for B-RAF^{WT}, B-RAF^{V600E}, B-RAF^{K601E} and B-RAFD^{D594V} atoms were 1.70 Å (SD = 0.13), 2.57 Å (SD = 0.27), 2.09 Å (SD = 0.26) and 1.82 Å (SD = 0.26), respectively (see Fig. 1A in Ref. [12] for details).

As described in detail in two recent publications, the two inter-linked water-mediated hydrogen bond networks (HBNs) identified in B-RAF^{WT}, remained stable throughout the MD simulation [15,16]. One of these HBNs (HBN1) was formed between Lys483, Glu501, Asp594, Gly596, Lys601, Ser607 and water molecules, and Asp594 and Lys601 were also a part of a second water-mediated HBN (HBN2) with Lys578, Asn581, Asp576 and Thr599. Thus a strong inter-linked HBN, in which the catalytic and A-loop residues are key components, was observed in the space between the αC-helix, the A-loop and the β6 strand in B-RAF^{WT} (see Fig. 1, and Fig. 2 in Ref. [16]).

Based on this analysis the average electrostatic interaction energy between the Lys483–Glu501 and the Lys601–Asp594 ion pairs in B-RAF^{WT} was estimated to a value of -70.8 ± 7.5 kcal/mol. The corresponding value for the interactions between the Lys601 and Glu501 residues was -93.8 ± 3.5 kcal/mol, comprising about 47% of the total A-loop–protein electrostatic interactions [16]. Similar results were obtained from previous analysis of a 10 ns MD simulation [15]. The strong interactions between Lys601 and the catalytic and ATP the coordinating residues Asp594, Glu501 and Lys483 suggest the important role of this lysine in the B-RAF^{WT} function and stability, which can explain the observed strong kinase activation in the presence of the K601E mutation. According to these results Lys601 interacts strongly with the ATP coordinating residues, thus it can potentially play a significant role in the inactive B-RAF^{WT} phosphorylation. A close contact between Asp594 and Lys601 was also detected in the crystal structure of the V600E mutant [5], indicating that our results are not affected significantly by the loop modelling.

The MD simulations results showed that the conformation and the electrostatic interactions between the residues joined to the HBN were different in the studied mutants. For instance, the strength of the electrostatic interaction energies that correspond to the interactions between the Lys483–Glu501 and the Lys601–Asp594 ion pairs in the wild type B-RAF were about 71.0 and 20.9 less negative in the V600E and K601E mutants than in the wild type, respectively [16]. These data demonstrate that the interactions between these ion pairs are strongly affected by the observed structural reorganisation within the ATP binding pockets of the mutants, which most likely affects the phosphorylation potential and kinase activation.

3.2. GRID analysis

In order to study the molecular basis of the experimentally observed mechanism of phosphorylation of the activation segment in B-RAF^{WT} and to explore the differences between the wild type kinase and the V600E, D594V and K601E mutants, we applied a GRID analysis. By GRID technique it is also possible to examine our hypothesis on the important role of Lys601 in relation to B-RAF activation [16] and to the phosphorylation specificity of the A-loop. This information can add to improved understanding of the processes of the B-RAF's phosphorylation and activation.

We use GRID maps to graphically illustrate the energetically favourable binding sites of the ATP molecule within the kinase binding pocket, by mapping the interactions between a given chemical sub-structure (a probe), and the protein residues. We used a PO_4H probe to identify the B-RAF residues that might react with a phosphate group provided by ATP, and therefore undergo phosphorylation. A detailed analysis of the specificity of the individual mutants was also performed. To investigate the contribution of the electrostatic forces to this process, a GRID calculation with a negative charged probe of −3 was run. Figs. 2–4 present the results from the GRID analysis for the B-RAF^{WT}, B-RAF^{D594V} and B-RAF^{V600E} kinase forms, and the corresponding results for B-RAF^{K601E} are found in Figure 1S in the supporting information.

In B-RAF^{WT}, only two possible phosphorylation sites were identified on the basis of the GRID analysis, one close to Thr599 and the second one was near Ser602 (see Fig. 2A). An interaction energy minimum between the probe and the protein residues of −21.1 kcal/mol was calculated. These results are in agreement with available experimental data, which indicate that the B-RAF^{WT} activation via the A-loop is only possible if mediated by phosphorylation of Thr599 and/or Ser602 [3]. Moreover, the Thr599 has been reported as the major A-loop phosphorylation site, whereas Ser602 is considered to be a relative minor one [3]. It has been speculated that these two residues are the only ones exposed to phosphorylation in the wild type form of B-RAF [4]. Our results confirm this hypothesis and thus we use the computational result to suggest a molecular basis for the observed phosphorylation specificity of the activation segment in B-RAF^{WT}. The GRID analysis relies entirely on the 3D geometry used for the proteins binding pocket, and that the model system gives a reasonable estimate of the flexibility of the A-loop. The good agreement between the modelling result and experimental data indicate that the 3D geometry used is of acceptable quality to form basis for such analyses.

According to our analysis, the strongest electrostatic protein–probe attractive force came from the Lys483 residue, possibly contributing to the phosphorylation of Thr599 (see Fig. 2B). Lys483 is well a conserved residue within the whole kinase family and it is thus unlikely to determine the phosphorylation specificity of B-RAF without the support of other more specific residues. A possible explanation of the observed B-RAF phosphorylation specificity, is that the positively charged Lys601 residue, which is not present in most of other kinases, Lys578 and Lys483 cooperatively generate strong attractive electrostatic force that potentially can favour the ATP transport to the kinase binding site and form specific phosphorylation pockets close to Thr599 and Ser602 (see Figs. 1 and 2A). Thus according to our calculations an energetically favourable phosphorylation region was identified between the residues involved in the HBN2 portion of the observed hydrogen bond network in B-RAF^{WT} (see Figs. 1 and 2A). As discussed before, Lys601 was involved in both HBN1 and HBN2 portions of the

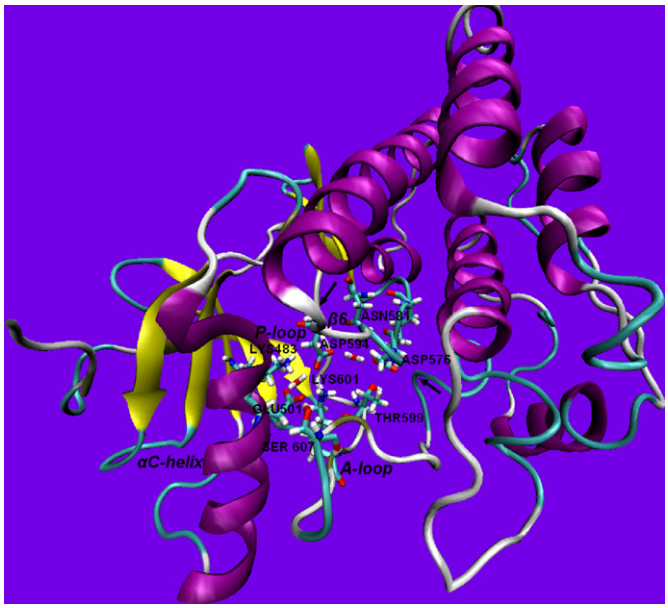

Fig. 1. Graphics showing the conformation of the identified hydrogen bond network (HBN), the protein sub-structures surrounding the HBN and the catalytic residues in B-RAF^{WT}, obtained from a 15 ns MD simulation. Key residues and protein sub-structures are marked specifically, with black arrows pointing at the beginning and the end of the activation segment (A-loop).

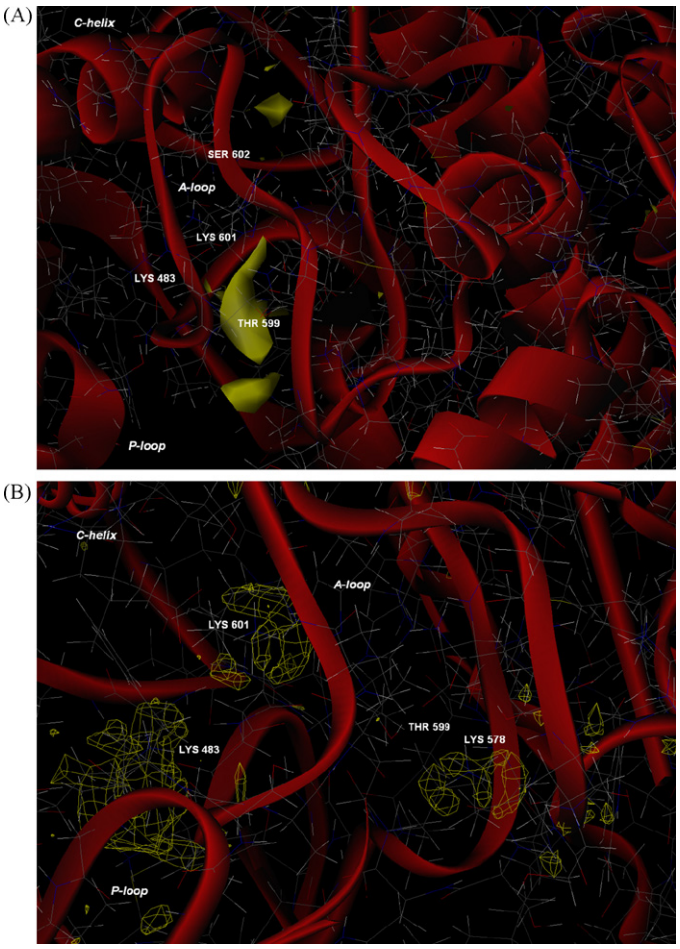

Fig. 2. GRID maps of the favoured ATP binding sites (level of −15.0 kcal/mol protein–probe interactions) in B-RAF^{WT} using the HPO_4 group (A) and the −3 dot charge (B) as probes. Potential ATP binding sites were identified close to Thr599 and Ser602, which is in agreement with experimental observations.

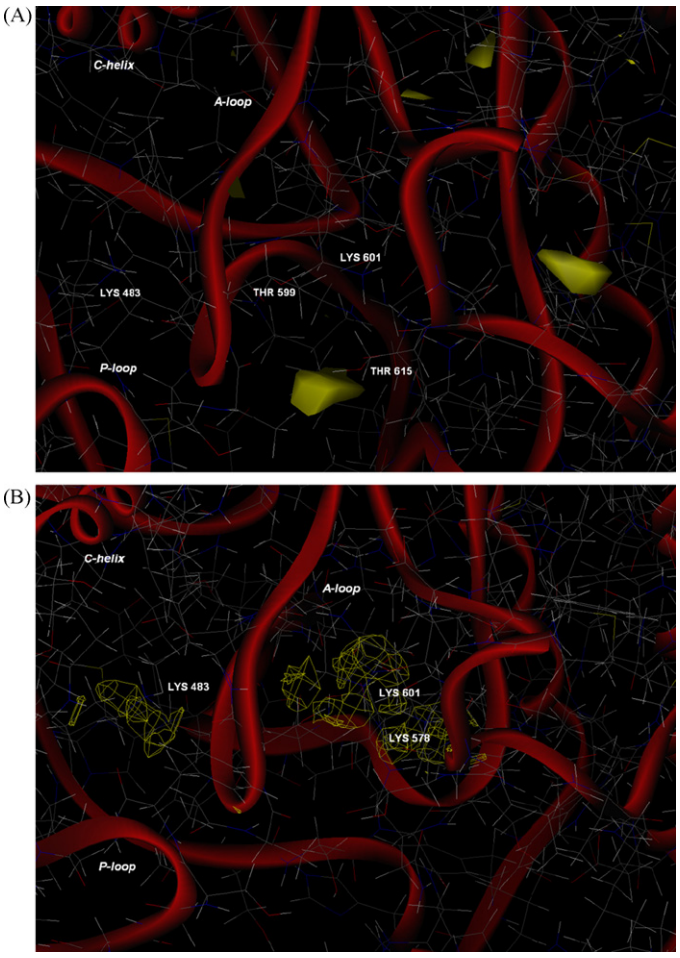

Fig. 3. GRID maps of the favoured ATP binding sites (level of −15.0 kcal/mol protein–probe interactions) in B-RAF^{D594V} using the HPO_4 group (A) and the −3 dot charge (B) as probes. For this impaired activity mutant, a potential ATP binding site was identified close to Thr615, but none is found in the vicinity of the catalytic residues.

identified hydrogen bond network in B-RAF^{WT}, forming a large cleft within HBN2 in which the Thr599 was joined [16], enabling ATP to access the potential phosphorylation region.

It has been demonstrated that the Lys483–Glu501 ion pair plays a significant role in ATP coordination, increasing the kinase activity compared to the kinases where this salt bridge was disrupted [27,9]. In our recent MD based analysis, salt bridges were also identified between Lys601 and Lys483 and Glu501 in B-RAF^{WT}. Furthermore, we argued that Lys601 plays an important role for the conformational stability of the A-loop in the unbounded B-RAF^{WT} and B-RAF^{V600E}, as well as for the ligand–protein interactions of these B-RAF forms in a complex with a ligand [15,16]. The Lys601 might thus play role in ATP coordination, and thus it is straightforward to speculate that this residue might act as a regulator of these processes. Based on these studies, which use detailed analysis of MD simulations and statistical analysis of the biological activity in relation to key energy contributions, as well as the GRID analysis presented here, we speculate that Lys601 can be considered as a specific B-RAF^{WT} catalytic residue. Further experimental studies are required to test this hypothesis

In contrast to B-RAF^{WT}, the major electrostatic forces in B-RAF^{D594V} were concentrated within the Lys601–Lys578 region, equally distributed on each of these lysines, and the Lys483 residue had a minor contribution. The most favourable phosphorylation site was observed at a larger distance from Thr599 and thus significant differences compared to B-RAF^{WT} were seen (see Fig. 3A and B). Due to the specific HBN reorganisation no phosphorylation pocket was indentified within the A-loop of this mutant with the GRID analysis. The most energetically favourable ATP binding region was found close to Thr615, which is placed at the end of the activation segment. Even after eventual phosphorylation of this residue, large conformational changes in the A-loop are not considered likely. Moreover, the calculated minimum of the protein–probe interaction energy was 2.2 kcal/mol more positive than the corresponding value for B-RAF^{WT}. Although the absence of potential phosphorylation sites cannot be concluded based on GRID analysis alone, the experimentally observed inactivity of the B-RAF^{D594V} mutant indicates that the phosphorylation of the activation segment in B-RAF^{D594V} mutant is unlikely. Thus our results suggest that the D594V mutation converts the B-RAF kinase to a conformation that neither favours activation nor phosphorylation, which is in agreement with experimental results [5].

These data support one of the hypotheses about the role of B-RAF^{D594V} in tumorigenesis, namely that it acts as a dominant-negative regulator to suppress the rampant ERK signalling [28]. In a recent experimental study it was seen that the Act3 phosphorylates B-RAF^{V600E} and decreases it's activity to the level that is required for the tumour development in melanoma [29], i.e. initially promoting activation of B-RAF, but the resulting high intense activation of MAPK pathway is seen to inhibit further tumour progression. Similarly, it is straightforward to speculate that the level of the MEK phosphorylation by B-RAF^{V600E} is dependent on the concentration of the V600E mutant. Thus we suggest that B-RAF^{D594V} presumably down regulates the overall

activity of the B-RAF^{V600E}–MEK pathway, as the production of this kinase-dead mutant ensures that part of available B-RAF cannot contribute to the phosphorylation and activation of B-RAF. This may in turn suppress the total MEK phosphorylation sufficiently to maintain optimal conditions for progression of the cancer.

The GRID analysis results for B-RAF^{WT} and B-RAF^{D594V} were in agreement available experimental observations, and our approach correctly identified the two experimentally observed phosphorylation sites for the wild type B-RAF. Thus it can be concluded that this simple approach can give additional insight into the molecular level processes related to phosphorylation.

Similar analyses were made for the two activating mutants, B-RAF^{V600E} and B-RAF^{K601E}. It has been suggested that B-RAF^{V600E} mutation mimics the phosphorylation step [2,6] and that B-RAF^{V600E} and other activating mutants like B-RAF^{K601E} can activate MEK without activation segment phosphorylation taking place [5,6]. Very little experimental evidence on the activation mechanism of the B-RAF^{K601E} mutation can be found in the literature. This mutant is a highly activating, but different from other activating mutants, as the RAF specific Lys601 residue in B-RAF^{K601E} is replaced with a Glu.

Potential A-loop phosphorylation sites were not identified for the B-RAF^{K601E} mutant by means of GRID analysis, see Figure 1SA and B in the supporting material. As discussed before, the mutation of Lys601 to Glu totally disordered the HBN. Consequently, the strong attractive electrostatic forces between Lys483 and Lys601 in B-RAF^{WT} were eliminated due to the formation of a salt bridge between Lys483 and Glu601 in B-RAF^{K601E}, inducing significant conformational changes within the B-RAF binding pocket [16]. Potential A-loop phosphorylation sites cannot be ruled out based on such analysis, as they rely on simulated 3D geometry of the binding pocket, particularly the A-loop conformation. These results suggest, that the MEK phosphorylation in the B-RAF^{K601E}–MEK system, takes place almost exclusively via a non-phosphorylation mediated activation of the activation segment, and thus it is possible that A-loop phosphorylation sites are absent for this mutant.

In the GRID analysis shown in Fig. 4A, many residues that might potentially phosphorylate were identified in B-RAF^{V600E}. The most favourable ATP binding region in the A-loop was identified close to the Ser605 and Ser607 residues, which is also the most accessible part of the activation segment. The minimum interaction energy obtained with the GRID calculation is −21.0 kcal/mol, which is similar to the corresponding value for B-RAF^{WT}. According to our analysis, the Thr599 and Ser602 were also identified as possible phosphorylation sites. Moreover, the analysis of the electrostatic attractive forces showed that the main contribution came from four residues, Lys601, identified as the most significant residue, Lys483, Arg575 and Lys578, potentially favouring ATP transport to different regions of the A-loop (see Fig. 4B). Thus, the electrostatic force distributions differ to both B-RAF^{WT} and B-RAF^{D594V}, indicating that their allocation is an important factor for the kinase phosphorylation specificity.

Both the experimental and theoretical studies suggest that the V600E mutation destabilises the activation segment such that it adopts an open-like conformation that activates ERK without phosphorylation of it's own A-loop [5,6,15,16] (see Figs. 4A and 7 in Ref. [15]). As mentioned above, Act3 mediated phosphorylation of Ser364 and Ser428 in B-RAF^{V600E} reduced its activity to a level that ensured optimal conditions for tumour development in melanoma, i.e. maintaining high B-RAF^{V600E}–MEK–ERK activation by regulating the activity of the V600E mutant [29]. These residues are in significant distance to the A-loop, and this particular process can therefore not explain the function of the phosphorylation sites identified with the GRID method for the V600E. They might, however, have some function in the activation process.

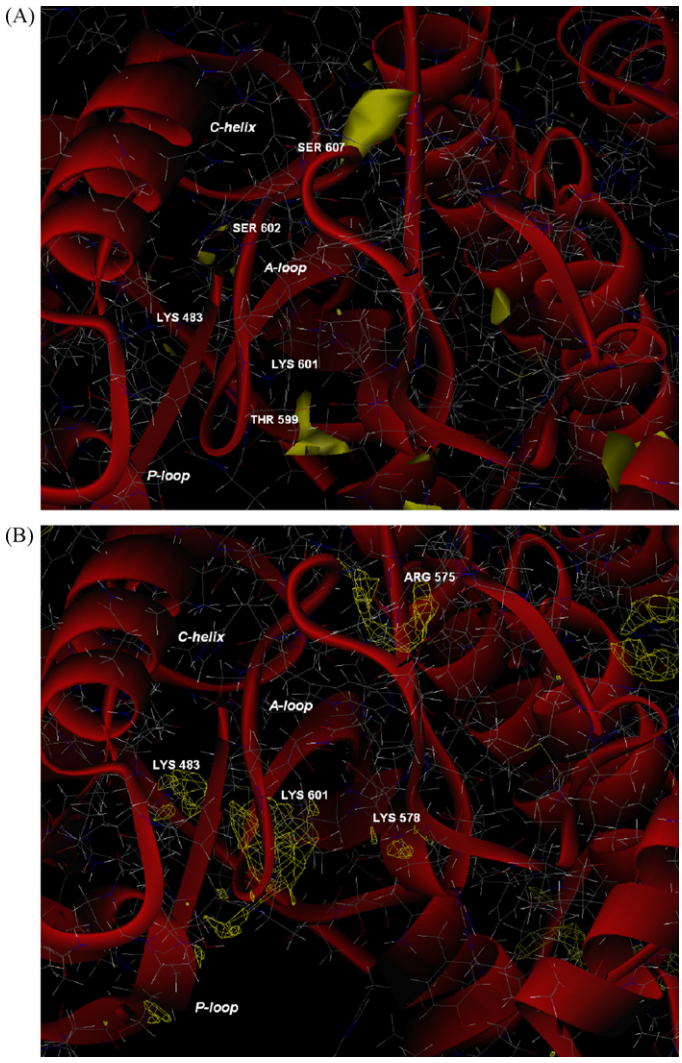

Fig. 4. GRID maps of the favoured ATP binding sites (level of −15.0 kcal/mol protein–probe interactions) in B-RAF^{V600E} using the HPO_4 group (A) and the −3 dot charge (B) as probes. Several potential ATP binding sites were identified for this high activity mutant, with the ones close to Ser607 and Thr599 being particularly interesting.

Thus the GRID results here indicate that the phosphorylation specificity might be different for the two of most frequently occurring cancer mutants, the very strongly activating B-RAF^{V600E} mutant and the strongly activating B-RAF^{K601E} mutant. It must be mentioned, that due to the A-loops structural flexibility it cannot be concluded that the B-RAF^{K601E} mutant does not have A-loop phosphorylation sites, only that they were not identified in our analysis. In the absence of experimental data, further conclusions on the phosphorylation specificity of these two mutants cannot be made. On the other hand, it was demonstrated that analyses based on a simple model system, could provide improved understanding of the molecular processes leading to phosphorylation of B-RAF^{WT} and B-RAF^{D594V}, and good agreement between experimental observations and modelling results was seen.

Acknowledgements

F. Fratev and S.Ó. Jónsdóttir acknowledge financial support from Danish Research Council for Technology and Production Sciences (FTP) and the Program Commission on Nanoscience, Biotechnology and IT (NABIIT). Thanks to I. Pajeva, O. Tabourea and E. Mihaylova for the helpful discussion.

Appendix A. Supplementary data

Supplementary data associated with this article can be found, in the online version, at doi:10.1016/j.jmgm.2009.12.005.

References

[1] M.J. Robinson, M.H. Cobb, Mitogen-activated protein kinase pathways, Curr. Opin. Cell Biol. 9 (1997) 180–186.
[2] H. Davies, G.R. Bignell, C. Cox, P. Stephens, S. Edkins, S. Clegg, J. Teague, H. Woffendin, M.J. Garnett, W. Bottomley, N. Davis, E. Dicks, R. Ewing, Y. Floyd, K. Gray, S. Hall, R. Hawes, J. Hughes, V. Kosmidou, A. Menzies, C. Mould, A. Parker, C. Stevens, S. Watt, S. Hooper, R. Wilson, H. Jayatilake, B.A. Gusterson, C. Cooper, J. Shipley, D. Hargrave, K. Pritchard-Jones, N. Maitland, G. Chenevix-Trench, G.J. Riggins, D.D. Bigner, G. Palmieri, A. Cossu, A. Flanagan, A. Nicholson, J.W. Ho, S.W. Leung, S.T. Yuen, B.L. Weber, H.F. Seigler, T.L. Darrow, H. Paterson, R. Marais, C.J. Marshall, R. Wooster, M.R. Stratton, P.A. Futreal, Mutations of the BRAF gene in human cancer, Nature 417 (2002) 949–954.
[3] B.H. Zhang, K.L. Guan, Activation of B-RAF kinase requires phosphorylation of the conserved residues Thr598 and Ser601, EMBO J. 19 (2000) 5429–5439.
[4] N.J. Dibb, S.M. Dilworth, C.D. Mol, Switching on kinases: oncogenic activation of B-RAF and PDGFR family, Nat. Rev. Cancer 4 (2004) 718–727.
[5] P.T. Wan, M.J. Garnett, S.M. Roe, S. Lee, D. Niculescu-Duvaz, V.M. Good, C.M. Jones, C.J. Marshall, S.J. Springer, D. Barford, R. Marais, Mechanism of activation of the RAF-ERK signaling pathway by oncogenic mutations of B-RAF, Cell 116 (2004) 855–867.
[6] A.E. Russon, E. Torrisi, Y. Bevelacqua, R. Perrotta, M. Libra, J.A. McCubrey, D.A. Spandidos, F. Stivala, G. Malaponte, Melanoma: molecular pathogenesis and emerging target therapies, Int. J. Oncol. 34 (2009) 1481–1489 (Review).
[7] O.M. Grbovic, A.D. Basso, A. Sawai, Q. Ye, P. Friedlander, D. Solit, N. Rosen, V600E B-Raf requires the Hsp90 chaperone for stability and is degraded in response to Hsp90 inhibitors, Proc. Natl. Acad. Sci. U.S.A. 103 (2006) 57–62.
[8] M. Malumbres, M. Barbacid, RAS oncogenes: the first 30 years, Nat. Rev. Cancer 3 (2003) 459–465.
[9] J.J. Liao, Molecular recognition of protein kinase binding pockets for design of potent and selective kinase inhibitors, J. Med. Chem. 50 (2007) 409–424.
[10] S. Moretti, V. De Falco, A. Tamburrino, F. Barbi, M. Tavano, N. Avenia, F. Santeusanio, M. Santoro, A. Macchiarulo, E. Puxeddu, Insights into the molecular function of the inactived mutations of B-raf involving the DFG motif, Biochim. Biophys. Acta 1793 (2009) 1634–1645.
[11] V. De Falco, R. Giannini, A. Tamburrion, C. Ugolini, C. Lupi, E. Puxeddu, M. Santoro, F. Basolo, Functional characterization of the Novel T599I-VKSRdel BRAF mutation in a follicular variant papillary thyroid carcinoma, J. Clin. Endocrinol. Metab. 93 (2008) 4398–4402.
[12] A.J. King, D.R. Patrick, R.S. Batorsky, M.L. Ho, H.T. Do, S.Y. Zhang, R. Kumar, D.W. Rusnak, A.K. Takle, D.M. Wilson, E. Hugger, L. Wang, F. Karreth, J.C. Lougheed, J. Lee, D. Chau, T.J. Stout, E.W. May, C.M. Rominger, M.D. Schaber, L. Luo, A.S. Lakdawala, J.L. Adams, R.G. Contractor, K.S. Smalley, M. Herlyn, M.M. Morrissey, D.A. Tuveson, P.S. Huang, Demonstration of a genetic therapeutic index for tumors expressing oncogenic BRAF by the kinase inhibitor SB-590885, Cancer Res. 66 (2006) 11100–11105.
[13] J. Tsai, J.T. Lee, W. Wang, J. Zhang, H. Cho, S. Mamo, R. Bremer, S. Gillette, J. Kong, N.K. Haass, K. Sproesser, L. Li, K.S. Smalley, D. Fong, Y.L. Zhu, A. Marimuthu, H. Nguyen, B. Lam, J. Liu, I. Cheung, J. Rice, Y. Suzuki, C. Luu, C. Settachatgul, R. Shellooe, J. Cantwell, S.H. Kim, J. Schlessinger, K.Y. Zhang, B.L. West, B. Powell, G. Habets, C. Zhang, P.N. Ibrahim, P. Hirth, D.R. Artis, M. Herlyn, G. Bollag, Discovery of a selective inhibitor of oncogenic B-Raf kinase with potent antimelanoma activity, Proc. Natl. Acad. Sci. U.S.A. 105 (2008) 3041–3046.
[14] P. Xie, C. Streu, J. Qin, H. Bregman, N. Pagano, E. Meggers, R. Marmorstein, The crystal structure of BRAF in complex with an organoruthenium inhibitor reveals a mechanism for inhibition of an active form of BRAF kinase, Biochemistry 48 (2009) 5187–5198.
[15] F. Fratev, S.Ó. Jónsdóttir, E. Mihaylova, I. Pajeva, Molecular basis of inactive B-RAF^{WT} and B-RAF^{V600E} ligand inhibition, selectivity and conformational stability: an *in silico* study, Mol. Pharm. 6 (2009) 144–157.
[16] F. Fratev, S.Ó. Jónsdóttir, An *in silico* study of the molecular basis of B-RAF activation and conformational stability, BMC Struct. Biol. 9 (2009) 47.
[17] H.M. Berman, J. Westbrook, Z. Feng, G. Gilliland, T.N. Bhat, H. Weissig, I.N. Shindyalov, P.E. Bourne, The Protein Data Bank, Nucleic Acids Res. 28 (2000) 235–242.
[18] M.A. Marti-Renom, A. Stuart, A. Fiser, R. Sánchez, F. Melo, A. Sali, Comparative protein structure modeling of genes and genomes, Annu. Rev. Biophys. Biomol. Struct. 29 (2000) 291–325.
[19] D.A. Case, T.A. Darden, T.E. Cheatham III, C.L. Simmerling, J. Wang, R.E. Duke, R. Luo, K.M. Merz, D.A. Pearlman, M. Crowley, R.C. Walker, W. Zhang, B. Wang, S. Hayik, A. Roitberg, G. Seabra, K.F. Wong, F. Paesani, X. Wu, S. Brozell, V. Tsui, H. Gohlke, L. Yang, C. Tan, J. Mongan, V. Hornak, G. Cui, P. Beroza, D.H. Mathews, C. Schafmeister, W.S. Ross, P.A. Kollman, AMBER 9, University of California, San Francisco, 2006.
[20] C.P. James, R. Braun, W. Wang, J. Gumbart, E. Tajkhorshid, .E. Villa, C. Chipot, R.D. Skeel, L. Kale, K. Schulten, Scalable molecular dynamics with NAMD, J. Comput. Chem. 26 (2005) 1781–1802.
[21] H.J. Berendsen, J. Grigera, T. Straatsma, The missing term in effective pair potentials, J. Phys. Chem. 91 (1987) 6269–6271.
[22] J.P. Ryckaert, G. Ciccotti, H.J.C. Berendsen, Numerical integration of the Cartesian equations of motion of a system with constraints: molecular dynamics of *n*-alkanes, J. Comput. Phys. 23 (1977) 327–341.
[23] T. Darden, D. York, L. Pederson, Particle mesh Ewald: an *N*.log(*N*) method for Ewald sums in large systems, J. Chem. Phys. 98 (1993) 10089–10092.
[24] W. Humphrey, A. Dalke, K. Schulten, VMD—Visual Molecular Dynamics, J. Mol. Graph. 14 (1996) 33–38.
[25] P.J. Goodford, A computational procedure for determining energetically favorable binding sites on biologically important macromolecules, J. Med. Chem. 28 (1985) 849–857.
[26] E. Carosati, S. Sciabola, G. Cruciani, Hydrogen bonding interactions of covalently bonded fluorine atoms: from crystallographic data to a new angular function in the GRID force field, J. Med. Chem. 47 (2004) 5114–5125.
[27] S.K. Hanks, T. Hunter, Protein kinases 6. The eukaryotic protein kinase superfamily: kinase (catalytic) domain structure and classification, FASEB J. 9 (1995) 576–596.
[28] M. Garnett, R. Marais, Guilty as charged B-RAF is a human oncogene, Cancer Cell 6 (2004) 313–319.
[29] M. Cheung, A. Sharma, S.V. Madhunapantula, G.P. Robertson, Akt3 and mutant V600E B-Raf cooperate to promote early melanoma development, Cancer Res. 68 (2008) 3429–3439.